ISSN 1063-7710, Acoustical Physics, 2024, Vol. 70, No. 3, pp. 409–415. © Pleiades Publishing, Ltd., 2024.

CLASSICAL PROBLEMS OF LINEAR ACOUSTICS AND WAVE THEORY

Peculiarities of Flexural Wave Propagation in a Notched Bar

A. A. Agafonov[a], M. Yu. Izosimova[a], R. A. Zhostkov[b], A. I. Kokshayskiy[a], A. I. Korobov[a, *], and N. I. Odina [a]

[a] *Moscow State University, Faculty of Physics, Moscow, 119991 Russia*

[b] *Schmidt Institute of Physics of the Earth, Russian Academy of Sciences, Moscow, 123995 Russia*

**e-mail: aikor42@mail.ru*

Received December 7, 2023; revised December 7, 2023; accepted April 24, 2024

Abstract—We present the results of numerical simulation and experimental studies of the propagation of flexural elastic waves in a notched metal bar with a rectangular cross section that approximates the acoustic black hole effect. The sample is a notched bar; the depth of notches increases according to a power law with an exponent of 4/3. The experimental results and the results of numerical simulation confirm that such bars slow the propagation velocity of an elastic wave towards the end of the bar. It is demonstrated that flexural waves in such structures exhibit dispersion and their amplitude at the end of the bar for some eigenfrequencies is higher than that in a solid bar. The eigenmode shapes of a solid and notched bar are compared together with the distribution of the flexural wave amplitude along the bars. The frequency dependence of the flexural wave length is studied during wave propagation towards the end of the notched bar.

Keywords: flexural waves in a bar, notched bar, acoustic black hole, laser vibrometry, numerical simulation, experiment

DOI: 10.1134/S1063771024601997

INTRODUCTION

Recently, researchers have shown interest in structures called “acoustic black holes” (ABHs) [1–3]. The main feature of such objects is that along a certain direction (depending on the structure geometry), the velocity of elastic waves decreases to zero, which should result in an infinite wave propagation time over a finite interval in space. The result is that there is no reflected wave as the incident wave propagates along this direction. In ABHs, such a reduction in the wave velocity is related to a reduction in local stiffness, which is usually achieved by modifying the geometry, e.g., by reducing the sample thickness according to a power law [4].

One of the first studies on ABHs was the fundamental work by M.A. Mironov [1], who considered the structure in the form of a thin plate, the thickness of which slowly changes to zero according to a power law. The law of the change (decrease) in the wavelength and increase in the amplitude in this structure was obtained.

The authors of review [5] consider the following types of ABHs: the so-called one-dimensional ABH in the form of a plate with a power-law profile; a spiral ABH; a bar with drilled pits decreasing in diameter [6]; a two-dimensional ABH; ABHs in the form of plates of varying thickness [8].

ABHs are interesting for structural acoustics and sound absorption, but in practice, they are only approximately implemented. The propagation of a flexural wave in samples made of various materials with a profile varying according to a power law is experimentally studied in [8–11]. In these studies, the effect of slowing of the Lamb flexural wave and increase in its amplitude as it approached the edge of a wedge was observed.

A modification of the ABHs in the form of a bar with a special law of the change in cross section is considered in [12, 13]. In these studies, the method and criteria for the applicability of the WKB (Wentzel–Kramers–Brillouin) approximation in the problem of transverse vibrations of a bar are also described in detail. The exact solutions obtained for a power-law dependence of the bar width and a quadratic dependence of the bar thickness on length were used to modify the WKB approximation for bars of constant width and arbitrarily changing thickness. Based on these solutions, expressions have been obtained for the input impedance matrix of a bar with a special law of the change in cross section.

The authors of [5] showed that structures acting as ABHs do not require high-quality manufacturing, which makes their production affordable. The authors of [4] note that this field has been insufficiently studied and requires a broadening of the possibilities of using ABHs.

An alternative to a plate or bar with a power-law profile is a notched bar [14], i.e., a bar with a rectangular cross section in which notches are cut normal to

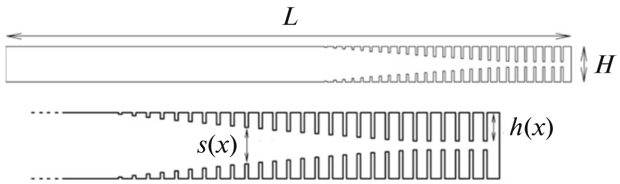

Fig. 1. Diagram of profile of a notched bar.

the bar axis and the depth of which increases according to a power law (Fig. 1). The local stiffness of such a bar decreases with an increase in notch depth. In particular, this structure is preferable because it does not require high-precision manufacturing of the bar end. If we compare the sizes of two similar types of ABHs, namely, a bar with a power-law profile and a notched bar with the same length, another advantage of the latter is that its critical frequency is reduced by five times compared to the more conventional ABHs with a power-law profile. The mass of the corresponding sample of the notched bar will be higher than that of the bar with a power-law profile. However, the author of [14] clarifies that the question of the number and location of notches remains open.

For a notched bar, it is impossible to obtain an exact analytical solution; therefore, to obtain the distribution of displacement fields, it is necessary to either simplify the problem or use numerical simulation. The author of [14] proposes using the commonly accepted equation of flexural oscillations of a bar nonuniform along its axis. As a result of calculations, a formula was obtained for the local thickness of the bar at the site of notches:

$$s(x) = H(x/L)^{\alpha},\ \alpha = \frac{4}{3}, \tag{1}$$

where $s(x)$ is the the gap width between opposite notches, H is the bar thickness, L is the length of the notched bar, and α is the exponent.

The bar begins to exhibit the characteristics of an ABH at frequencies above the critical frequency:

$$\omega = \sqrt{\frac{E}{12\rho}}\frac{3}{4}\frac{H}{L^2}. \tag{2}$$

Here, E is the Young's modulus and ρ is the density of the bar material.

For this type of ABHs, there are insufficient experimental studies and modeling results. In this study, we present the results of numerical simulation and experimental studies of the peculiarities of the propagation of flexural elastic waves in a notched bar with a rectangular cross section and notch depth varying according to power law (1), as well as with a gradually decreasing distance between notches. In addition, it is compared a control notch-free sample.

NUMERICAL SIMULATION

Here, two bars with dimensions of 3.9 × 6.8 × 200 mm were studied: a control notch-free sample and a sample with 28 notches. The distance from the free end of the bar to the center of the corresponding notch was set by the following expression:

$$x_i = \frac{2}{3}\frac{i}{N}(L-5) + \frac{1}{3}\left(\frac{i}{N}\right)^{7/3}(L-5), \tag{3}$$

where $i = \{1, 2, \ldots N\}$, $N = 28$ is the number of notches and L is the length of the notched part. According to (1), the depth was varied according to a power law:

$$h(x) = \frac{H - s(x)}{2},$$
$$s(x) = \max\left(H\left(\frac{x}{L}\right)^{4/3},\ 0.85\ \text{mm}\right).$$

Here, the formula for $s(x)$ is artificially limited to the minimum thickness to prevent fracturing of the samples upon their physical realization. The total length of the bar L_0 = 200 mm, the length of the notched part L = 90 mm, H = 6.8 mm, Z = 3.9 mm (the bar width) (Fig. 1).

The sample dimensions were selected based on the operating frequency range (in this study from 10 to 100 kHz) and a set of the following conditions:

(a) the approximation of a thin bar (the length should be several times higher than the transverse dimensions of the bar, and in the selected frequency range, only zero flexural modes should occur in the notch-free part);

(b) according to (2), the critical frequency of the ABH should correspond to the operating range of the source of acoustic waves (according to (2), for a bar with the given dimensions, the critical frequency is 942 Hz);

(c) the size of the notch-free part should make it possible to distinguish several wavelengths in the selected range.

The width of the notches is 0.75 mm (these are the minimum technically possible dimensions). Coordinate x_i is counted from the edge of the bar to the middle of the notch. The inner parts of notches are rounded (d = 0.75 mm).

The elastic characteristics of the sample material correspond to D16 grade duralumin: the density is 2680 kg/m^3, the propagation velocity of longitudinal waves is 6400 m/s, and that of transverse waves is 3130 m/s. Piezoceramic elements with longitudinal polarization were considered as the acoustic wave sources (Fig. 2a), mounted at the end of the bar in a notch-free zone on opposite surfaces of the bar and operating in phase opposition: the density is 4700 kg/m^3, the velocity of longitudinal waves is 6562 m/s, and that of transverse waves is 3582 m/s.

Numerical simulation of possible oscillatory processes in the ABH model was achieved using the finite element method in the COMSOL Multiphysics 5.3

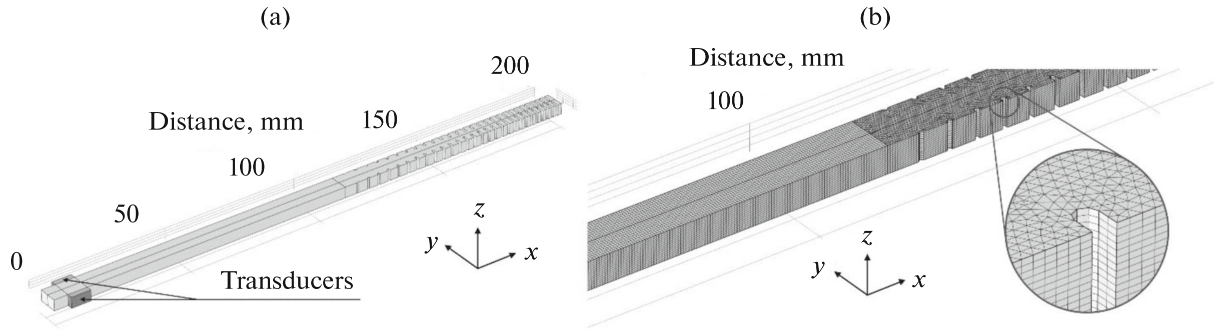

Fig. 2. (a) Example of set geometry of sample, (b) finite element mesh.

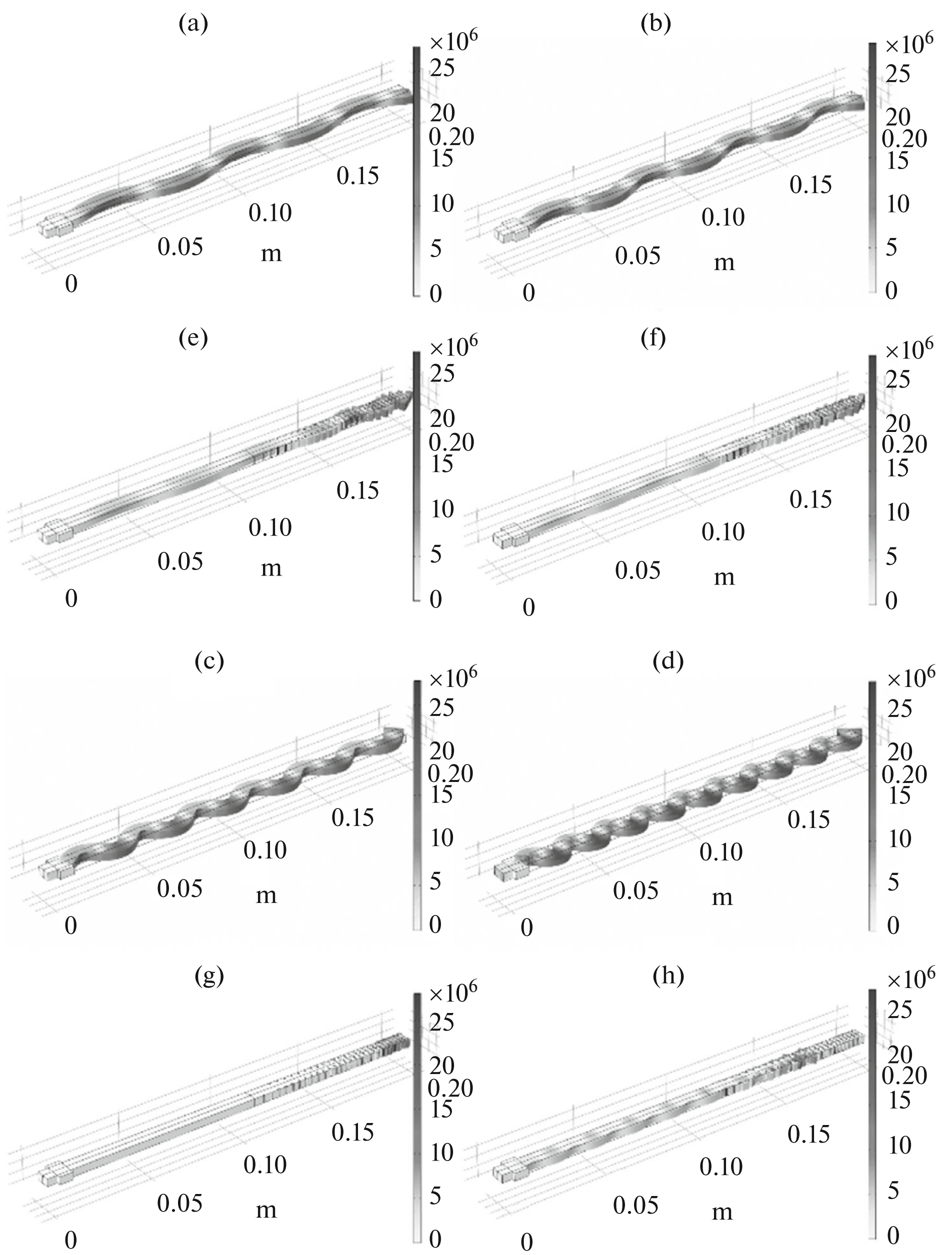

Fig. 3. Examples of shapes of flexural oscillations of bars in horizontal projection: control sample at frequencies (a) 12.8, (b) 22.7, (c) 54.6, and (d) 99.9 kHz; notched bar at frequencies (e) 10.4, (f) 21.8, (g) 52.9, and (h) 99.5 kHz.

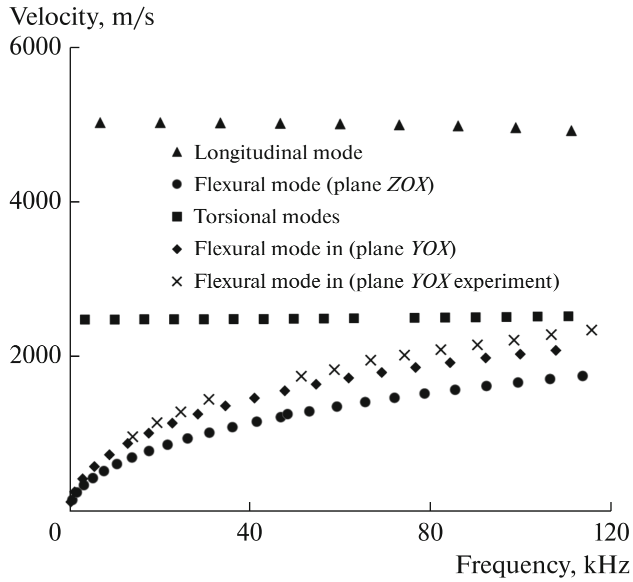

Fig. 4. Dispersion curves of notch-free bar (error of experimentally obtained data is less than size of symbol and increases from 2 to 9% with decreasing velocity).

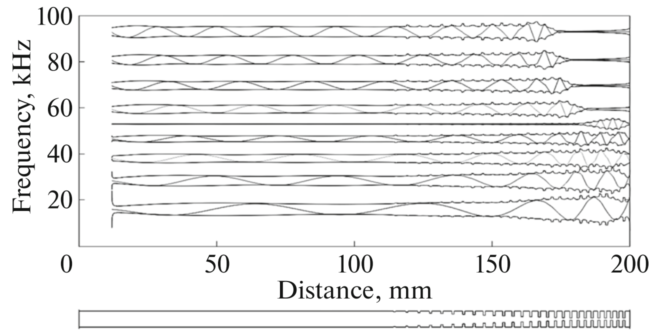

Fig. 5. Amplitude distribution of flexural mode in notched bar.

software code (license no. 9600341) with the connected Structural Mechanics unit. Numerical simulation was done using the approach of determining eigenfrequencies in a three-dimensional formulation without using any symmetry, since this option makes it possible to identify all possible types of oscillations. In the studied samples, four types of such oscillations are observed: a longitudinal and a torsional modes, and two flexural modes in different projections.

The boundary conditions of the model corresponded to the free outer edges of the sample, except for the outer boundaries of the piezoceramic elements, the coordinates of which were fixed.

The mesh of finite elements (Fig. 2b) was separately constructed in two regions: in the notch-free sample part close to the piezoceramic elements, a structured mesh of elements in the form of rectangular parallelepipeds was used, and the region with notches was filled with elements in the form of triangular prisms. The size of these elements was certainly much smaller than the studied wavelengths; therefore, it was determined by the features of the geometry and was of 0.05–0.1 of the height/width of the sample, namely, 0.35–0.39 mm. The total number of elements was about 400 000 (a slight deviation from this number was due to variations in the notch structure in samples). This choice of finite element mesh allowed an accuracy in estimatinng eigenfrequencies of up to 50 Hz.

The solution to the problem was reached by studying the eigenfrequencies in the 0–100 kHz range. For

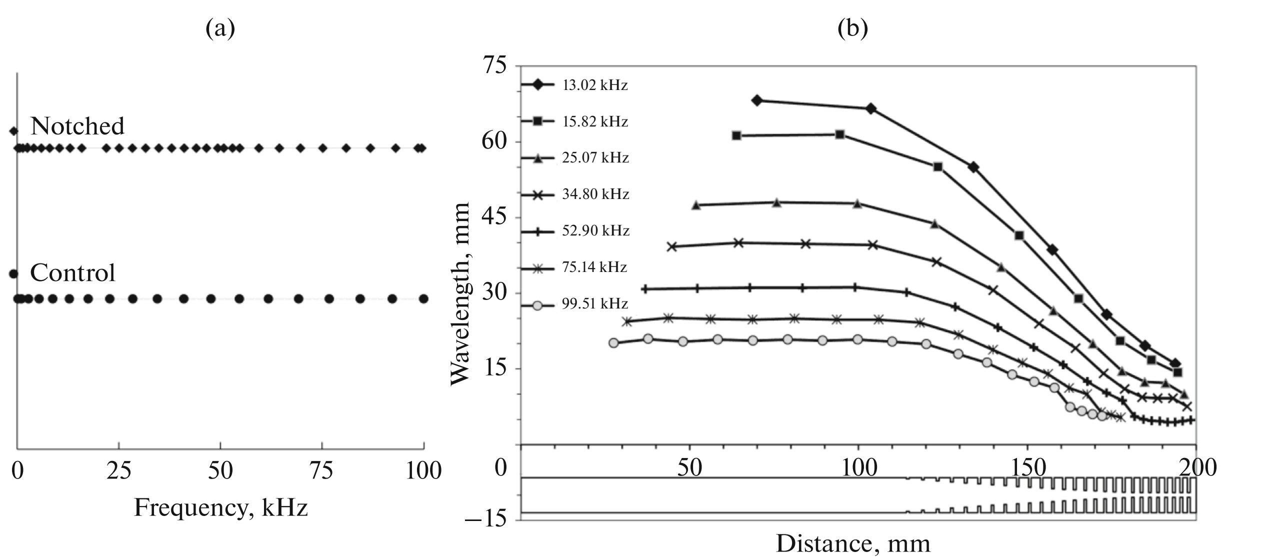

Fig. 6. (a) Eigenfrequencies of flexural mode propagating in notched and control bars. (b) Dependence of flexural wavelength on distance to free end in frequency range from 10 to 100 kHz. Under plot is profile of a notched bar, which corresponds to x coordinates.

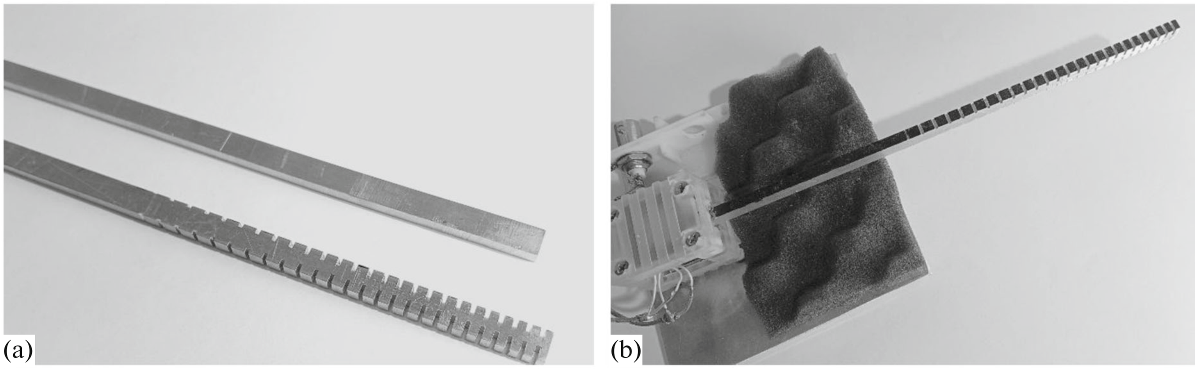

Fig. 7. (a) Samples of bars, (b) mounting of sample and transducers.

further analysis, we used the components of particle displacement on the notched surface of the sample as a function of the coordinate and a graphical representation of the shape of oscillations (Fig. 3).

As expected, the distribution of the oscillation amplitude along the control bar is uniform over its entire length regardless of frequency; the wavelength also does not change with distance to the end of the bar (Figs. 3a–3d). Based on the simulation results for this bar, the dispersion curves were calculated for all modes in the frequency range from 100 Hz to 100 kHz (Fig. 4).

For the notched bar, a series of distributions of the normalized amplitude of the displacement of the horizontal flexural mode along the sample was plotted as a function of the distance to the free end of the bar with envelopes following the profile of the notched bar (Fig. 5). The Hilbert transform was used to calculate the functions orthogonal to the original modes, and to reconstruct the shapes of their envelopes. Frequencies are plotted along the y-axis, where the zero amplitude of mode oscillations corresponds to its eigenfrequency. Amplitudes are normalized to the initial value of each curve. The profile of the notched bar is shown below the x-axis.

After crossing the interface between the uncut and cut parts of the bar, the wavelength decreases as it approaches the free end; i.e., the ABH effect occurs. In this case, the shape of its envelope follows the profile of the notched bar. In addition, at frequencies above 52.9 kHz, closer to the end of the bar, the half-wavelength becomes comparable with the distance between notches, and the wave stops to reach the end of the bar. It should be noted that, despite the fact that the flexural wavelength acts similarly to the Lamb wavelength in a plate with a parabolic profile [11], the amplitude slightly increases except for the boundary mode at a frequency of 52.9 kHz, when the amplitude increases by ten times.

Figure 6a shows the spectra of the eigenfrequencies of the control and notched bars in the range of up to 100 kHz. The spectrum of the notched bar is more enriched than that of the control sample. This is explained by that as the flexural wave approaches the end of the notched rod, the wavelength decreases (Fig. 6b), and a larger number of wavelengths for a similar frequency fits the notched part (Fig. 3).

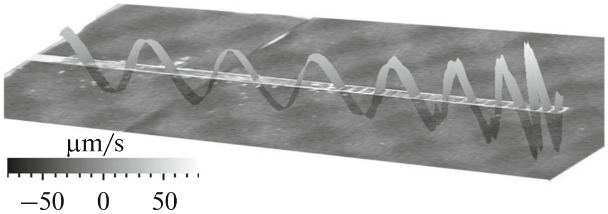

Fig. 8. Example of visualization of surface oscillation of notched bar recorded using a scanning vibrometer.

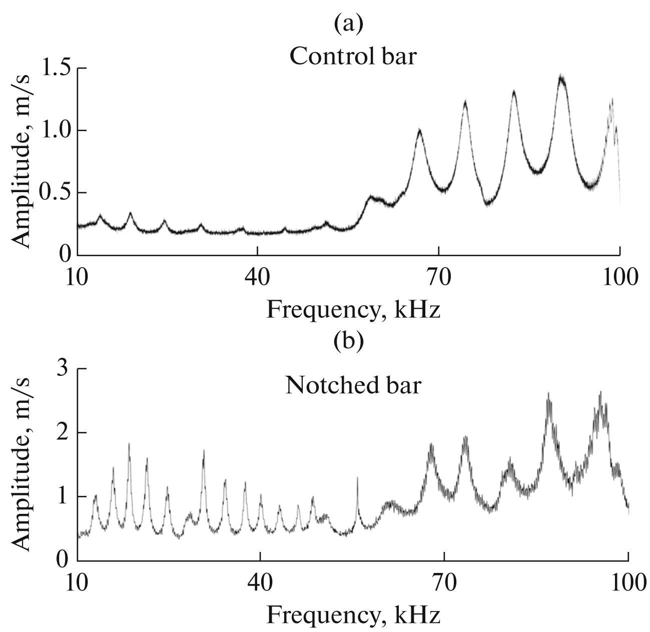

Fig. 9. Amplitude-frequency response of (a) control and (b) notched bar in frequency range from 10 to 100 kHz.

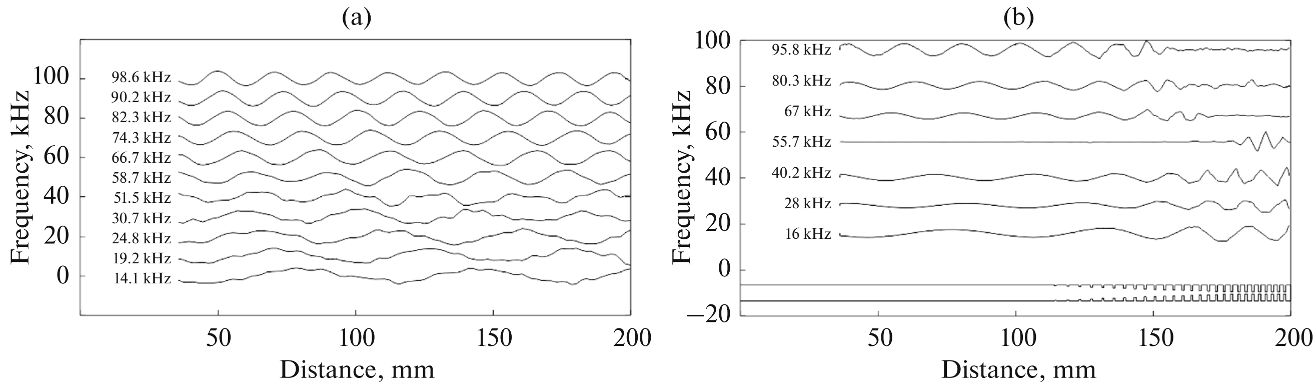

Fig. 10. Amplitude distribution of flexural mode in (a) control and (b) notched bar.

A similar decrease in the wavelength in a notched bar and its tendency to a fixed value was predicted in [14] and is due to a gradual decrease in the local stiffness of the bar. The wavelength and corresponding velocity do not reach zero at the end of the bar due to that it was decided to limit the minimum thickness of the gap between notches to 0.85 mm for the possibility of further physical implementation of such a sample.

EXPERIMENTAL

For experimental studies, two samples of bars with dimensions of 3.9 × 6.8 × 200 mm were made of D16 alloy: a notch-free control bar and notched bar (Fig. 7a).

The experimental studies were performed using a setup developed for the study of a wedge with a parabolic profile [11]. The sample was held at the uncut end by a specially designed mounting system (Fig. 7b). Two piezoelectric transducers were attached on opposite sides of the sample. At the four corner points of the clamp, rigid clamping of the sample is provided by screw fastening. The transducers are spring-loaded with a soft material and are not involved in the mounting system, but provide boundary conditions. The inner planes of the transducers are shifted in phase opposition in a piston mode in such a way that a flexural wave is excited in the sample.

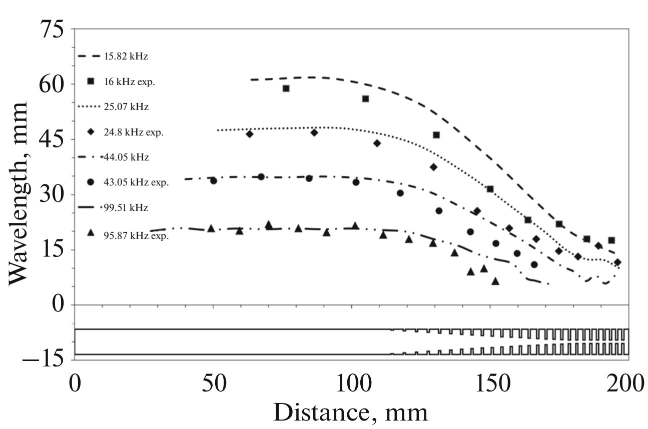

Fig. 11. Dependence of flexural wavelength in bar on distance to free end in frequency range from 10 to 100 kHz. Curves, simulation results; points, experimental data.

A Polytec PSV-300 laser scanning vibrometer was used to scan the surface of the notched bar in such a way that the image of the vertical displacement of the surface (Fig. 8) obtained using a laser vibromometer upon the experiment corresponds to the bending of bars in the horizontal plane in Fig. 3. Scanning was performed only for some frequencies to make sure that the conditions of a thin bar in this frequency range are fulfilled. Then, the values of the amplitude of the vibrational velocity were determined at the selected points on the centerline of the surface. The number of points was selected in such a way that the spatial resolution was sufficient for visualization of the wave, namely, at least five points per half-wavelength.

At the beginning of the experiment, the amplitude–frequency response was measured for each of the samples in a continuous sweep mode in the range from 10 to 100 kHz (Fig. 9).

The distribution of the eigenfrequencies of samples is similar to the pattern of the spectra obtained as a result of modeling (Fig. 6a). In the control sample at frequencies from 55 kHz and above, more efficient generation of eigenfrequencies occurs. The amplitude distribution along the bar is more uniform taking into account the nodes and crests of standing waves than at low frequencies (Fig. 10a). At the same time, the wavelength does not depend on the distance along the bar, and the dispersion curve for this bar qualitatively repeats the shape of a simulated curve plotted using numerical simulation (Fig. 4).

In the notched bar, the spectrum is "smoothed"; i.e., the amplitudes of resonance modes at frequencies below 55 kHz are comparable to the amplitude of the peaks at higher frequencies. The pattern of the oscillation amplitude of a flexural wave in a notched bar (Fig. 10b) qualitatively replicates the modeling results: as it approaches the end of the rod the wavelength decreases, and as soon as the distance between the notches becomes equal to the half-wavelength, the wave does not propagate further (Fig. 5). Only a slight shift in the frequency spectrum (±3 kHz) is observed compared to the simulated one (Fig. 5). The simulated and experimentally obtained values of the flexural wavelength in a notched bar as a function of the distance to the end of the bar are presented in Fig. 11 for different frequencies. Closer to the end of the bar, the error in determining the wavelength increases from 1 to 4 mm.

For all studied frequencies, a decrease in the flexural wavelength in the bar is observed as a function of the passed distance. However, at a distance of about 30 mm from the end, there is almost no decrease in the wavelength and even a nonmonotonic behavior of the wavelength as a function of the distance is observed, because this bar has five notches at the end, which are equal in depth. The discrepancy between the modeling results and the results of experimental studies may be due to inaccuracy in the manufacture of the bar (including making notches), incorrect accounting for the location and method of mounting.

CONCLUSIONS

In this study, we present the results of simulation and experiment, which confirm the appearance of the ABH effect in the range from 1 to 100 kHz in a notched bar, the depth of the notches in which varies according to power law (1). In addition, the results are compared with a control notch-free sample. For this purpose:

(1) a sample of a notched bar with 28 notches was calculated and made of a D16 aluminum alloy; the distance between notches decreases towards the end of the bar and their depth increases according to (1);

(2) a numerical method was used to simulate the propagation of a flexural wave in the notched and notch-free bars;

(3) laser vibrometry was used to visualize the distribution of the vibrational velocity amplitude in the samples as a function of the distance to the end of the bar in the frequency range from 10 to 100 kHz.

For all studied modes, a decrease in the flexural wavelength in the bar as a function of the passed distance is observed. However, a change in the wavelength in the vicinity of the end is step-wise due to both the presence of notches of equal depth at the end of the bar and to the effects of coincidence or mismatch of the flexural wavelength in the bar with the sizes of the cut pieces. Therefore, the mode at 52.9 kHz (numerical simulation) and at 55.7 kHz (experiment) stands out, the wavelength of which sharply decreases and reaches an average value of about 4.8 mm at a distance of 8 mm from the end.

The results of the studies provide information on the peculiarities of the propagation of flexural waves in notched bars and can be useful in developing noise-damping devices based on them.

FUNDING

This study was supported by the Russian Science Foundation, project no. 19-12-00098. Numerical simulation was done within the state assignment of the Schmidt Institute of Physics of the Earth, Russian Academy of Sciences.

CONFLICT OF INTEREST

The authors of this work declare that they have no conflicts of interest.

REFERENCES

1. M. A. Mironov, Sov. Phys. Acoust. **34** (3), 318 (1988).
2. V. V. Krylov and A. L. Shuvalov, Proc. Inst. Acoust. **22** (2), 263 (2000).
3. V. V. Krylov, Moscow Univ. Phys. Bull. **45** (6), 65 (1990).
4. V. V. Krylov and F. J. B. S. Tilman, J. Sound Vib. **274** (3-5), 605 (2004).
5. A. Pelat, F. Gautiera, S. C. Conlon, and F. Semperlotti, J. Sound Vib. **476**, 115316 (2020).
6. O. Guasch, M. Arnela, and P. Sánchez-Martín, J. Sound Vib. **395**, 65 (2017).
7. V. V. Krylov, IEEE Trans. Ultrason. Ferroelectr. Freq. Control **61** (8), 1296 (2014).
8. J. J. Bayod, J. Vib. Acoust. **133** (6), 061003 (2011).
9. H. Ji, J. Luo, J. Qiu, and L. Cheng, Mech. Syst. Signal Process. **104**, 19 (2018).
10. D. J. O'Boy, V. V. Krylov, and V. Kralovic, J. Sound Vib. **329**, 4672 (2010).
11. A. A. Agafonov, A. I. Korobov, M. Yu. Izosimova, A. I. Kokshaiskiy, and N. I. Odina, Acoust. Phys. **68** (5), 415 (2022).
12. M. A. Mironov, Acoust. Phys. **63** (1), 1 (2017).
13. M. A. Mironov, in *Proc. 9th All-Union Acoustic Conf.* (Leningrad, 1991), p. 23 [in Russian].
14. M. A. Mironov, Acoust. Phys. **65** (6), 634 (2019).

Translated by N. Podymova